Leadership in Sustainable Infrastructure
Leadership en Infrastructures Durables

Vancouver, Canada
May 31 – June 3, 2017/ *Mai 31 – Juin 3, 2017*

MODELING OF HYDRAULIC AND WATER QUALITY PERFORMANCE OF BIORETENTIION CELLS

Huang, Jian[1], He, Jianxun[1,3], Chu, Angus[1] and Valeo, Caterina[2]
[1] University of Calgary, Canada
[2] University of Victoria, Canada
[3] jianhe@ucalgary.ca

Abstract: The use of Low Impact Development (LID) technologies for managing urban stormwater runoff has shown promise in reducing or eliminating the need of traditional stormwater infrastructure. Bioretention cells, also called rain gardens, are one type of LID that collects, stores and treats stormwater runoff on site. To date, few models are available for simulating the behavior of bioretention cells. Therefore, this paper proposed an event-based model for predicting hydraulic and water quality performance of bioretention cells. The model was developed using the data collected from a field-scale bioretention cell located in the City of Calgary, Alberta. A total of eight storm events were used in model calibration and validation. The performance of the model was assessed in terms of both hydraulic parameters including time to peak, peak flow, and volume reduction, and water quality parameter - the removal efficiency of total suspended solids (TSS). The results demonstrate that the proposed model is capable of capturing the temporal variation of hydraulic performance of bioretention and simulating outflow hydrographs with the coefficient of determination (R^2) above 0.77 and the normalized root-mean-square deviation (*NRMSD*) ranging from 8.5% to 15.6%. The percent errors between measured and modeled hydraulic and water quality parameters have a maximum value of 10.0%. As a result, the proposed model has great potential as a practical modeling tool for assessing the performance of bioretention cells and designing.

1 INTRODUCTION

Urbanization has led to an increase of stormwater runoff as natural land surfaces are being replaced by impervious surfaces such as roads, buildings, parking lots, and many other urban infrastructures. The continuous increase of stormwater runoff potentially challenges the capacity of existing stormwater infrastructures and jeopardizes urban water environment (Lee and Bang 2000, Muthanna et al. 2008). Bioretention cells, also called rain gardens, are one of Low Impact Development (LID) technology and offers a practical solution to manage increasing stormwater runoff. When surface runoff is routed to bioretention cells, they provide temporary detention and promote infiltration so that the stormwater runoff volume and peak can be potentially attenuated (Davis et al. 2009, Trowsdale and Simcock 2011). The existing body of knowledge demonstrates the effectiveness of bioretention in delaying the time to peak and reducing the runoff peak and volume (Davis 2008, Hunt et al. 2008, Khan et al. 2012a). Previous studies also demonstrate that bioretention cells can substantially reduce the concentrations of total suspended solids (TSS), nutrients and heavy metals. Their removal efficiency was found to be associated with several variables including inflow pollutant concentration, magnitude of the storm event, as well as environment temperature (Braga et al. 2007, Hatt et al. 2009, Hsieh and Davis 2005, Khan et al. 2012b).

In the literature, many previous studies have primarily focused on assessing bioretention performance through analyzing and interpreting field and laboratory observations. There are also a few studies that have

utilized several modeling techniques (e.g., data-driven and physically-based models and commercial software) to simulate the hydraulic and/or water quality performance of bioretention cells. For instance, Brown et al. (2013) employed an agricultural drainage model to simulate the water storage of bioretention cells. Palhegyi (2009) developed a water balance model to estimate water storage and assist in sizing bioretention cells. Khan et al. (2013) developed a regression model to predict the outflow of bioretention. He and Davis (2010) applied Richard's equation to simulate flow through bioretention cell using a finite element model built on the platform of COMSOL Multiphysics. In addition, Akan (2013) adopted the Green Ampt equation to model water movement within a bioretention cell. To date, very few studies have been conducted to model water quality performance of bioretention cells. The water quality modeling has been particularly focused on TSS removal by a soil or gravel layer. Yao et al. (1971) proposed a physically-based model for a gravel media, which is actually a rapid sand filter, to simulate the major governing removal mechanisms including sedimentation, interception and diffusion. Wu (1994) developed a model to simulate TSS removal by a gravel media given a constant water pressure head. Wong et al. (2006) introduced a first order kinetic decay model to estimate the overall TSS removal by a gravel media. Most recently, Li and Davis (2008) utilized the classical macroscopic depth filtration model to simulate TSS removal by individual layers of a bioretention cell. No study has been found to apply the developed methodologies from filter units to model TSS removal by bioretention, regardless of the recognition of their similarity in TSS removal.

The majority of previous studies on hydraulic modeling for bioretention primarily addressed a particular variable such as runoff storage, flow through layers, or water balance; while the water quality models have mostly been developed for gravel or soil media individually instead for an entire bioretention cell, which often consists of both soil and gravel layers. Due to the popularity of bioretention, several municipalities in Canada have formulated design standards for bioretention cell, which use reduction of peak flow and runoff volume, delay in time to peak, and TSS removal as design criteria (e.g., Greater Vancouver Sewerage & Drainage District 2012, The City of Calgary 2011, Toronto and Region Conservation Authority 2010). Thus, there is a need to develop a modeling tool that can provide comprehensive information to aid in engineering design of bioretention. To fulfill the need, the objectives of this paper are to: 1) develop a modeling tool that can simulate both hydraulic and water quality performance of bioretention for assisting in its design, and 2) to validate the model by applying it to a bioretention cell, which was tested in a field study conducted in the City of Calgary, Canada.

2 MODEL DEVELOPMENT

A bioretention cell usually consists of multiple soil layers, which have various particle sizes for rooting of vegetation, and a gravel layer often with an under-drain lying underneath of the soil layers. The soil layers are designed with high porosity to promote infiltration; while the gravel layer is added not only to provide temporary storage for infiltrated water but also to support the upper soil layers and the under-drain (Roy-Poirier et al. 2010). Flow movement within, and sediment removal by the soil and gravel layers can be modeled based on the same theory considering their individual particle sizes and porosities. In this paper, the model developed for permeable pavements by Huang et al. (2016) was adopted and further revised to model the performance of bioretention cells, considering their similarity in structure and mechanisms governing flow and TSS removal. The conceptual scheme of the model is shown in Figure 1, while the flow chart of the model is illustrated in Figure 2. The model was briefly described below and detailed information about the model can be found in Huang et al. (2016). The model was developed for receiving both direct precipitation and runoff from surrounding area.

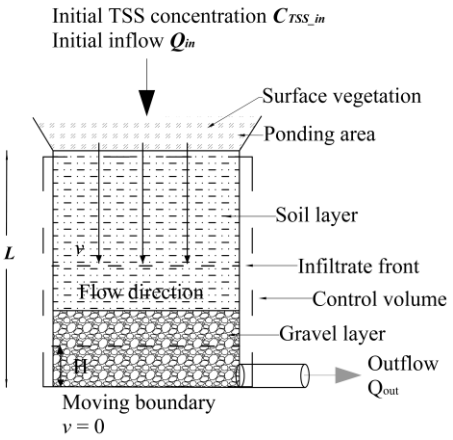

Figure 1. Conceptual scheme of the hydraulic model

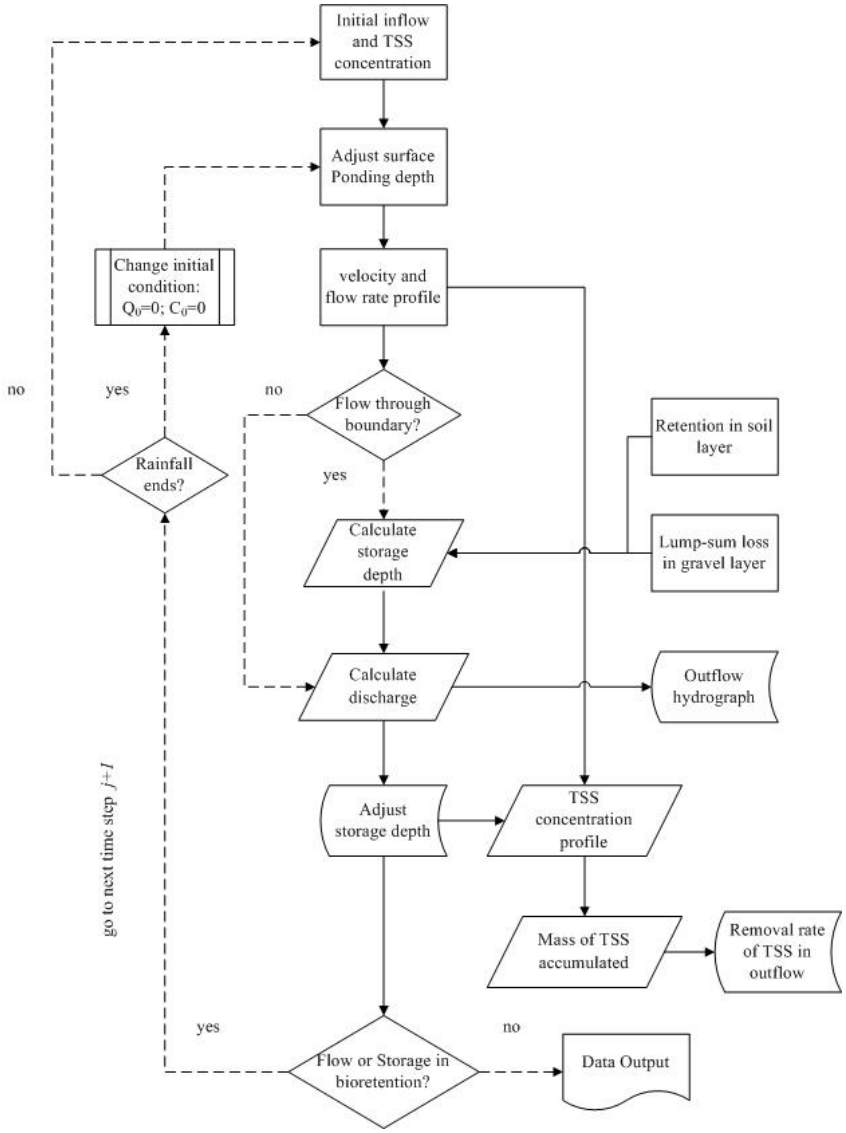

Figure 2. Flow chart of the model

2.1 Flow and sediment removal equations

The modified Kozeny-Carman equation (Eg. 1) is employed to simulate the infiltrated flow through a bioretention cell. The infiltrated flow, which moves downward, is assumed to be vertical and outflow is generated when the downward moving water front reaches the under-drain (Figure 1).

[1] $$\frac{\partial v}{\partial L} = \frac{1}{180}\frac{m^3}{(1-m)^2}\cdot(\varphi d)^2\cdot\frac{g}{\mu L}$$

where v is the vertical flow velocity through the soil and gravel layers [m/s]; m is the porosity of soil or gravel layers; φ is the sphericity of particle, which ranges from 0 to 1 depending on the shape of particle; d is the particle diameter [m]; g is the gravitational acceleration [m/s^2]; μ is the kinematic viscosity of infiltrated water [m^2/s]; and L is the depth of bioretention cell [m].

Yao et al. (1971) developed a sediment removal model for sand filter media in water and wastewater treatment processes. This model is utilized to simulate the processes of sediment removal by the soil and gravel layers of bioretention cell.

[2] $$\frac{\partial C}{\partial L} = -\frac{3}{2}\frac{(1-m)}{d}\alpha\left[0.9\left(\frac{kT}{\mu d_p dv}\right)^{2/3} + \frac{3}{2}\left(\frac{d_p}{d}\right)^2 + \frac{(\rho_p-\rho)g{d_p}^2}{18\mu v}\right]C$$

where C is the concentration of TSS [mg/L]; and α represents contact efficiency, which is the number of contacts that succeed in producing adhesion divided by the number of collisions that occur between suspended particles and soil or gravel layer. The coefficient α ranges from 0 to 1; while ideally α equals to 1 if the suspended particles are completely mixed in water. k is Boltzmann constant (1.3805×10-23 J/K); T is absolute temperature of stormwater [K]; d_p and ρ_p are the diameter [m] and the density [kg/m^3] of particle; and ρ is the density of infiltrated water [kg/m^3].

2.2 Numerical approximation

The finite difference approximation is applied to solve Eqs. 1 and 2. The numerical calculation of v is given in details below, while the calculation of TSS removal can be found in Huang et al. (2016).

The velocity, v [m/s], at the time step j is expressed by:

[3] $$v_{i+1}^{j} = v_i^j + \frac{1}{180}\cdot\frac{{m_i}^3}{(1-m_i)^2}\cdot(\varphi d_i)^2\cdot\frac{g}{\mu L}\Delta L$$

where the subscript i is the section number after discretization of the depth of bioretention cell L; and ΔL represents the distance between sections i and $i+1$.

During a storm event, a bioretention cell undergoes a "filling process" as stormwater runoff continuously enters the ponding area for temporary detention. At the same time, water in the ponding area starts to infiltrate the soil and/or gravel layers. When infiltrated water exceeds the storage limit of the cell, namely reaching the under-drain, excess water is discharged out of the cell. The storage depth, from the top of the cell to the boundary, where $v = 0$, moves either upward or downward (Figure 1). The surface ponding depth at time step j can be estimated based on the ponding depth at the previous time step $j-1$ and the change of ponding depth under the current time step j:

[4] $${D_{pond}}^{j} = {D_{pond}}^{j-1} + a\cdot D_{in}^{j} - D_{out}^{j}$$

where D_{pond} represents the ponding depth [m]; a is the water loss coefficient due to interception by vegetation on the top of the bioretention cell; D_{in} and D_{out}, which are the inflow and infiltrated water depths [m], respectively. D_{in} and D_{out} at time step j are calculated by:

[5] $${D_{in}}^{j} = {Q_{in}}^{j}\Delta t/A$$

[6] $${D_{out}}^{j} = {f_0}^{j}\Delta t$$

where A represents the surface area of the bioretention cell [m^2]; Δt represents the time interval between time step j and $j+1$ [s]; f_0 is the surface infiltration rate of the soil layer [m/s]; and Q_{in} is the inflow rate [m/s].

When infiltrated water flows through the cell, a portion of infiltrated water is retained by the soil layer. The amount of water retained is dependent on the field capacity and antecedent moisture level of the layer. The depth of water retained within the layer (D_{soil}) is expressed by:

[7] $$D_{soil}{}^{j} = \begin{cases} \frac{v_b^j \cdot \Delta t \cdot L_{soil}}{m_{soil} \cdot L}, & \sum_1^j D_{soil} < \text{cap} \cdot L_{soil} \cdot \theta_{initial} \\ 0, & \sum_1^j D_{soil} \geq \text{cap} \cdot L_{soil} \cdot \theta_{initial} \end{cases}$$

where v_b represents flow velocity near the bottom [m/s]; L_{soil} is the depth of the soil layer [m]; m_{soil}, cap and $\theta_{initial}$ denote the porosity [m^3/m^3], the filled capacity [m^3/m^3] and the antecedent moisture level of the soil layer, respectively. Eq. 7 implies that infiltrated water is retained in the soil layer before its field capacity is reached.

Since gravel merely retains water due to its physical nature, a water loss coefficient b is used to take account of the lump-sum loss when water moves through the gravel layer (D_{gravel}).

[8] $$D_{gravel}{}^{j} = \frac{b \cdot v_b^j \cdot \Delta t \cdot L_{gravel}}{m_{gravel} \cdot L}$$

where L_{gravel} and m_{gravel} are the depth [m] and the porosity [m^3/m^3] of the gravel layer.

Then the storage depth (H [m]) in the bioretention cell at time step j can be estimated based on the storage depth at the previous time step $j-1$ and the change of water storage (in depth) under the current time step j:

[9] $$H^j = H^{j-1} + h_{in}^j - h_{out}^j - D_{soil}^j - D_{gravel}^j$$

[10] $$h_{in}^j = {v_b^j \Delta t}\Big/{m_{gravel}}$$

[11] $$h_{out}^j = {Q_{out}^j \Delta t}\Big/{A \cdot m_{gravel}}$$

[12] $$Q_{out}^j = \delta A_{pipe} \sqrt{2gH^{j-1}}$$

where h_{in} and h_{out} are the infiltrated water depth [m] that is ready for discharge and the water depth [m] discharged from the under-drain pipe, respectively; Q_{out} represents the outflow rate from the sub-drain pipe [m^3/s]; δ and A_{pipe} are the transient loss coefficient and the cross-sectional area of the under-drain pipe (0.008 m^2 in the paper), respectively for calculating Q_{out}.

3 SITE DESCRIPTION AND DATA COLLECTION

The pilot-scale bioretention cell is located in Currie Barracks, a residential area in the southwest of Calgary. As the cell was constructed for testing purposes only, it does not receive any stormwater runoff from its adjacent areas. The cell is 32 m^2 in surface area (8.0 m long and 4.0 m wide). Vegetation sits on the mulched surface layer which is 75 mm deep. Major types of vegetation include *Salix bebbiana*, *prunus pensylvanica* and *potentilla fruticosa*. This layer along with the surface ponding area can provide a temporary detention up to 200 mm. The cell consists of a 300 mm upper rooting zone, a 600 mm deep rooting zone, and a 300 mm gravel layer from the top to the bottom. The upper and deep rooting zones have similar soil types (70% of sand and 30 % of silt and clay) and particle characteristics. Thus, these two zones were treated together in the model and referred to as the “soil layer". The gravel layer consists of 40 mm drainage rocks and a 100 mm diameter under-drain leading to an adjacent monitoring manhole. The underlying soil is fairly impermeable as it has a measured infiltration rate of 0.58 mm/hr. In addition, woven-geotextile is placed between the soil and gravel layers to separate and stabilize the two layers. A layer of non-woven geotextile was installed to prevent pollutant migration to the underlying soil. Thus, water loss due to infiltration into the underlying soil was considered negligible.

Bioretention cells are considered as a part of major drainage system, which should provide a service level for 100-year storm event (The City of Calgary 2011). The hydraulic and water quality data collected in eight 100-year storm events, which were simulated considering the impervious to pervious ratio of 4. The simulations were conducted from August 2008 to July 2009 and were used to calibrate and validate the developed model. In each simulated event, street sediments were added to stormwater withdrawn from a nearby stormwater pond to simulate the stormwater runoff from an urban catchment with various TSS levels. Outflow from the under-drain was continuously monitored and soil moisture was measured at several depths to capture soil moisture levels prior to each event. Table 1 summarizes inflow characteristics including intensity (i) and duration (t) of each storm event, event mean TSS concentration ($C_{TSS\text{-}in}$), antecedent soil moisture of the soil layer ($\theta_{initial}$), and water temperature (T). Table 1 also shows the outflow characteristics including peak flow (Q_p), time to peak (t_p), volume (V_{out}), volume reduction (VR), modeled event mean TSS concentration ($C_{TSS\text{-}out}$), and TSS removal efficiency (R_{TSS}).

Table 1. Inflow and outflow characteristics observed in each simulated storm event

Test No.	Test date	Inflow characteristics					Outflow characteristics					
		i (mm/hr)	t (min)	$C_{TSS\text{-}in}$ (mg/L)	$\theta_{initial}$	T (°C)	Q_p (L/s)	t_p (min)	V_{out} (L)	VR (%)	$C_{TSS\text{-}out}$ (mg/L)	R_{TSS} (%)
1	06/08/2008	134.29	21	33	0.307	26.4	0.039	96	52	99.31	13	99.73
2	15/08/2008	80.58	36	290	0.328	25.4	0.105	70	239	96.91	15	99.84
3	27/08/2008	96.08	31	292	0.308	24.1	0.270	116	575	92.76	15	99.63
4	07/10/2008	90.77	34	295	0.410	11.6	0.166	42	396	95.19	20	99.67
5	24/10/2008	95.16	32	111	0.430	14.3	0.232	50	728	91.03	8	99.35
6	09/06/2009	119.46	27	206	0.315	18.3	0.290	92	897	89.57	20	98.99
7	08/07/2009	92.59	34	135	0.385	21.1	0.188	54	403	95.20	7	99.75
8	22/07/2009	81.69	36	128	0.334	19.5	0.180	74	477	93.92	19	99.10

4 MODEL CALIBRATION AND VALIDATION

4.1 Model calibration

In the model, several parameters require estimation. Some of these parameters can be obtained from field measurements, whereas others are determined through model calibration due to a lack of information and/or difficulty in measuring in the field. These parameters are selected or determined as following:

- Δt and ΔL are selected to ensure the stability of numerical results.
- The kinematic water viscosity is determined according to measured T of inflow.
- φ is set as 0.25 and 0.1 for soil particle and gravel, respectively, according to their shape.
- Based on inflow particle size distribution (PSD) (Khan et al. 2012b), d_p of 120 μm is used.
- From lab measurements, ρ_p is approximately 1,090 kg/m^3.
- δ is in the range of [0 1] and is determined through model calibration.
- a and b are initially assumed to be 0.05 and 0.08, respectively, and their further calibration may be needed in model calibration.
- cap is estimated to be 0.275 m^3/m^3 (Khan et al. 2012a).
- m_{soil}, which is not a constant, is determined as a function of the operation time of the cell in the model calibration as it is expected to vary with time due to the deposition of solids in the layer; whereas m_{gravel} is treated as a constant (0.4) due to the absence of obvious external loading (e.g., traffic), which could lead to the degradation of m_{gravel} (Huang et al. 2016).

The eight simulated storm events (Table 1) were divided into two groups: Events 1, 3, 5, 6 and 8 for the model calibration and Events 2, 4 and 7 for the model validation. Before the model calibration, sensitivity analyses were performed to identify the acceptable ranges of the calibration parameters. The model was then calibrated manually using the trial-and-error approach. In the model calibration, the parameters were determined to yield acceptable percent errors (e.g., less than 10%) in a variety of modeled hydraulic and

water quality variables. The model performance was also evaluated using two statistical metrics: determination coefficient (R^2) and normalized root-mean-square deviation (*NRMSD*).

The simulated and measured outflow hydrographs are presented in Figure 3 for Events 3 and 6 as examples. In the model calibration, R^2 ranges from 0.84 to 0.93; while *NRMSD* is in the range between 9.65% and 14.08%. These results indicate a good agreement between the measured and simulated flows in all calibration events. Table 2 presents the percent errors between measured and simulated hydraulic and water quality variables for each calibration event. As shown in Table 2, the parameters were calibrated to ensure that the errors are less than 10%. The calibrated δ is 0.68, and the values of a and b remain at 0.05 and 0.08, respectively.

The degradation of m_{soil} was identified in the model calibration. Furthermore, m_{soil} can be described as a function of the operation time (t_o) since Event 1. The relationship between m_{soil} and t_o developed based on the model calibration was expressed as Eq. 13. The calibrated relationship was then applied in the model validation to determine m_{soil} of each validation event.

[13] $$m_{soil} = -0.006t_o + 34.79 \qquad (R^2 = 0.98)$$

where t_o is in the unit of day.

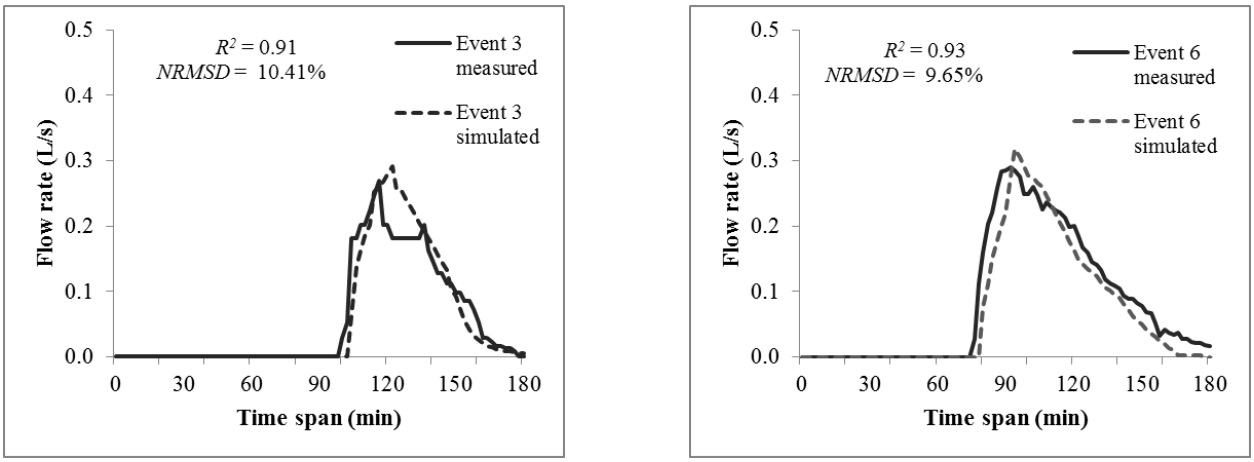

Figure 3. Measured and simulated outflow hydrographs of Events 3 and 6 in the model calibration

Table 2. Percent errors between measured and simulated variables in the model calibration

Event	Parameter	Error (%)	Event	Parameter	Error (%)	Event	Parameter	Error (%)
1	Q_p (L/s)	5.13	3	Q_p (L/s)	7.78	5	Q_p (L/s)	6.03
	t_p (min)	6.25		t_p (min)	5.17		t_p (min)	8.00
	V_{out} (L)	1.92		V_{out} (L)	4.52		V_{out} (L)	-8.79
	VR (%)	-0.01		*VR* (%)	-0.35		*VR* (%)	0.87
	R_{TSS} (%)	-2.90		R_{TSS} (%)	-6.34		R_{TSS} (%)	-3.84
6	Q_p (L/s)	10.00	8	Q_p (L/s)	10.00			
	t_p (min)	2.17		t_p (min)	8.11			
	V_{out} (L)	-9.70		V_{out} (L)	-9.64			
	VR (%)	1.13		*VR* (%)	0.62			
	R_{TSS} (%)	-6.28		R_{TSS} (%)	-3.10			

4.2 Model validation and discussion

The m_{soil} of Events 2, 4 and 7 is estimated to be 34.7%, 34.4% and 32.8%, respectively, based on the calibrated relationship between m_{soil} and t_o (Eq. 13). Figure 4 presents the measured and simulated outflow hydrographs of Event 4 as an example in the model validation. The percent errors between measured and simulated hydraulic and water quality variables are shown in Table 3. The calculated errors of all hydraulic and water quality variables are all less than 10%. In the model validation, R^2 ranges from 0.77 to 0.95, while *NRMSD* varies in the range between 8.48% and 15.64%.

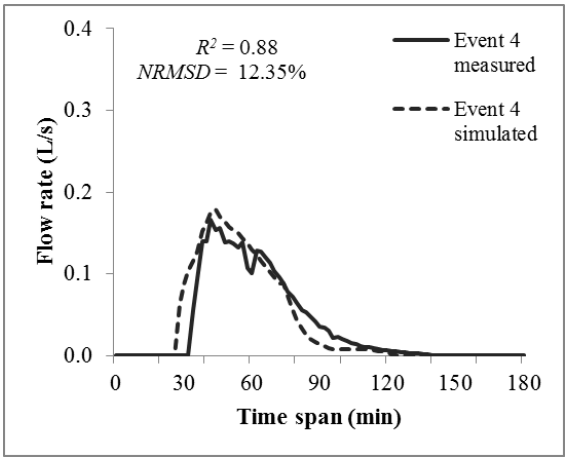

Figure 4. Measured and simulated outflow hydrographs of Event 4 in the model validation

Table 3. Percent errors between measured and simulated variables in the model validation

Parameter	Error (%) in Event 2	Error (%) in Event 4	Error (%) in Event 7
Q_p (L/s)	-4.76	7.83	5.85
t_p (min)	8.57	9.52	-9.26
V_{out} (L)	-8.37	6.06	-5.96
VR (%)	0.27	-0.31	0.30
R_{TSS} (%)	-5.48	-6.74	-4.05

The model validation shows that the calibrated model can simulate each validation event and is especially capable of capturing the temporal variation of the hydraulic performance of the bioretention cell. As shown in the outflow characteristics in Table 1, the hydraulic performance of the cell, in general, tends to degrade with time, as Q_p and V_{out}, and consequently *VR* increase whereas t_p decreases with time. The results might be ascribed to the decrease of m_{soil} with t_o as illustrated in the model calibration results shown in Figure 5. However, the recovery of the hydraulic performance was observed in the last two events, Events 7 and 8. The results from both the model calibration and validation clearly show that the proposed model effectively predicted the variation of hydraulic variables, which can be ascribed to the effects of the combination of the porosity of the soil layer and the antecedent moisture levels of each simulated event.

For a bioretention cell, physical properties such as porosity and antecedent moisture level, are not stationary over time. The developed model successfully captured the dynamics of hydraulic performance of the cell. This result strongly suggests that the model is applicable for modeling long-term hydraulic performance of bioretention cells. The model, however, currently applies the model calibration process to establish the influence of the porosity of the soil layer on operation time. In addition, the field measurements provide information on the moisture level prior to an event. In order to make the model more generalized, a model is required to capture the temporal variation of the porosity of the soil layer and the antecedent soil moisture levels and combine it with the developed model. The model was developed based on field

observations in 100-year storm events, thus, model verification under different magnitude events is recommended. Furthermore, several municipalities define the level of service for TSS at a specified particle size range; therefore, further model improvements to account for PSD is also recommended.

5 CONCLUSION

This paper developed a physically-based model for bioretention cells. The results proved its applicability by applying it to simulate both hydraulic and water quality (TSS removal) performance of a bioretention cell in Calgary. More importantly, the proposed model successfully captured the temporal variation, especially of the hydraulic performance, which is characterized by peak flow, time to peak, and volume reduction. Thus the model is of practical value in aiding in the engineering design of bioretention. In order to generalize the model for wider application, further research is recommended on several issues, such as modeling temporal variation of porosity and antecedent moisture levels, further verifying for other magnitude storm events, and taking in account PSD when modeling TSS removal.

ACKNOWLEDGEMENT

The authors would like to thank Mitacs Elevate program and Westhoff Engineering Resources Inc. for the financial support. The authors also would like to acknowledge the contribution of Dr. Usman Khan (York University) during his MSc at the University of Calgary in data collection.

REFERENCES

Akan, A.O. 2013. Preliminary design aid for bioretention filters. *Journal of Hydrologic Engineering*, **18**(3): 318-323.

Braga, A., Horst, M. and Traver, R. G. 2007. Temperature effects on the infiltration rate though an infiltration basin BMP. *Journal of Irrigation and Drainage Engineering*, **133**(6), 593-601.

Brown, R.A., Skaggs, R.W. and Hunt, W.F. 2013. Calibration and validation of DRAINMOD to model bioretention hydrology. *Journal of Hydrology*, **486**: 430-442.

Davis, A.P. 2008. Field performance of bioretention: Hydrology impacts. *Journal of Hydrologic Engineering*, **13**(2): 90-95.

Davis, A.P., Hunt, W.F., Traver, R.G. and Clar, M. 2009. Bioretention technology: an overview of current practices and future needs. *Journal of Environmental Engineering*, **135**(3): 109-117.

Greater Vancouver Sewerage & Drainage District. 2012. Stormwater source control design guidelines. Vancouver (Canada.)

Hatt, B.E., Fletcher, T.D. and Deletic, A. 2009. Hydrologic and pollutant removal performance of biofiltration systems at the field scale. *Journal of Hydrology*, **365**(3-4): 310-321.

He, Z. and Davis, A.P. 2010. Process modeling of storm-water flow in a bioretention cell. *Journal of Irrigation and Drainage Engineering*, **137**(3): 121-131.

Hsieh, C.H. and Davis, A.P. 2005. Evaluation and optimization of bioretention media for treatment of urban storm water runoff. *Journal of Environmental Engineering*, **131**(11): 1521-1531.

Huang, J., He, J., Valeo, C. and Chu, A. 2016. Temporal evolution modeling of hydraulic and water quality performance of permeable pavements. *Journal of Hydrology*, **533**: 15-27.

Hunt, W.F., Smith, J.T., Jadlocki, S.J., Hathaway, J.M. and Eubanks, P.R. 2008. Pollutant removal and peak flow mitigation by a bioretention cell in urban Charlotte, N. C. *Journal of Environmental Engineering*, **134**(5): 403-408.

Khan, U.T., Valeo, C., Chu, A. and van Duin, B. 2012a. Bioretention cell efficacy in cold climates: Part 1—hydrologic performance. *Canadian Journal of Civil Engineering*, **39**(11): 1210-1221.

Khan, U.T., Valeo, C., Chu, A. and van Duin, B. 2012b. Bioretention cell efficacy in cold climates: Part 2—water quality performance. *Canadian Journal of Civil Engineering*, **39**(11): 1222-1233.

Khan, U.T., Valeo, C., Chu, A. and He, J. 2013. A Data Driven Approach to Bioretention Cell Performance: Prediction and Design. *Water*, **5**(1): 13-28.

Lee, J.H. and Bang, K.W. 2000. Characterization of urban stormwater runoff. *Water Research*, **34**(6): 1773-1780.

Li, H. and Davis, A.P. 2008. Urban particle capture in bioretention media. II: Theory and model development. *Journal of Environmental Engineering*, **134**(6): 419-432.

Muthanna, T.M., Viklander, M. and Thorolfsson, S.T. 2008. Seasonal climatic effects on the hydrology of a rain garden. *Hydrological Processes*, **22**(11): 1640-1649.

Palhegyi, G.E. 2009. Modeling and sizing bioretention using flow duration control. *Journal of Hydrologic Engineering*, **15**(6): 417-425.

Roy-Poirier, A., Champagne, P. and Filion, Y. 2010. Review of bioretention system research and design: past, present and future. *Journal of Environmental Engineering*, **136**(9): 878-889.

The City of Calgary. 2011. Stormwater management and design manual. Wastewater and Drainage.

Toronto and Region Conservation Authority. 2010. Low impact development stormwater management planning and design guide. Toronto (Canada.)

Trowsdale, S.A. and Simcock, R. 2011. Urban stormwater treatment using bioretention. *Journal of Hydrology*, **397**(3): 167-174.

Wong, T.H., Fletcher, T.D., Duncan, H.P. and Jenkins, G.A. (2006). Modelling urban stormwater - a unified approach. *Ecological Engineering*, **27**(1): 58-70.

Wu, Y. 1994. An analysis of constant-pressure filtration. *Chemical Engineering Science*, **49**(6): 831-836.

Yao, K.M., Habibian, M.T. and O'Melia, C.R. 1971. Water and waste water filtration: concepts and applications. *Environmental Science and Technology*, **5**(11): 1105-1112.